Magnetocaloric effect and refrigeration capacity in Gd60Al10Mn30 nanocomposite

Stéphane Gorsse, Bernard Chevalier, Glenn Orveillon

Magnetocaloric effect and refrigeration capacity in Gd 60 Al 10 Mn 30 nanocomposite

S. Gorsse, B. Chevalier, and G. Orveillon

Citation: Applied Physics Letters **92**, 122501 (2008); doi: 10.1063/1.2884326
View online: http://dx.doi.org/10.1063/1.2884326
View Table of Contents: http://scitation.aip.org/content/aip/journal/apl/92/12?ver=pdfcov
Published by the AIP Publishing

Magnetocaloric effect and refrigeration capacity in $Gd_{60}Al_{10}Mn_{30}$ nanocomposite

S. Gorsse,[a] B. Chevalier, and G. Orveillon
Institut de Chimie de la Matière Condensée de Bordeaux, ICMCB, CNRS, Université Bordeaux 1, 87 Av. Dr A. Schweitzer, 33608 PESSAC Cedex, France

(Received 1 November 2007; accepted 27 January 2008; published online 25 March 2008)

The magnetic behavior, magnetocaloric effect (MCE), and refrigeration capacity of the $Gd_{60}Al_{10}Mn_{30}$ metallic glass containing nanocrystallites of Gd are investigated. It is found that the temperature dependence of the magnetization exhibits multiple second-order magnetic transitions due to the composite effect. The resulting magnetic entropy change and adiabatic temperature change compare well with MCE of known magnetic refrigerants. A high refrigeration capacity of 660 J kg^{-1}, a large operating temperature range around 150 K and a soft magnetic behavior make this nanocomposite an attractive candidate as magnetic refrigerants in a temperature range where pure Dy is the best material currently available. © *2008 American Institute of Physics*.
[DOI: 10.1063/1.2884326]

Magnetocaloric effect (MCE) is the heating or the cooling of magnetic solids in a varying magnetic field.[1] Adiabatic magnetization of a material gives rise to an increase of its temperature while a cooling results of an adiabatic demagnetization. Magnetization/demagnetization cycles are then similar to compression/expansion of a gas and can be used for cooling. Magnetic refrigeration based on MCE attracts very much attention because it is an environmentally friendly and high energy efficiency cooling technology.[2]

MCE results of the isothermal magnetic entropy change ΔS_M upon the application of a magnetic field, due to the coupling of magnetic spins with the magnetic field. The adiabatic temperature change ΔT_{ad} is due to an increase (or a decrease) of the lattice vibration entropy resulting of the variation of the sum of the lattice and electronic entropies by the opposite sign of ΔS_M under adiabatic magnetization (or demagnetization) of the material. ΔS_M and ΔT_{ad} are proportional to the size of the magnetic moments and the strength of the applied field.

A good solid refrigerants is a magnetic materials exhibiting: (i) a high density of magnetic moments (high concentration of $4f$ and/or $3d$ elements), (ii) a strong temperature and field dependence of the magnetization (occurrence of a magnetic phase transformation around the working temperature), and (iii) high permeability and reduced magnetic hysteresis to avoid energy losses during the magnetization/demagnetization cycles.

Families of magnetic materials which exhibit large MCE values include the rare-earth (RE) intermetallics REM_2 (M=Al, Co, and Ni),[3] $Gd_5(Si_{1-x}Ge_x)_4$,[4] $Mn(As_{1-x}Sb_x)$,[5] $MnFe(P_{1-x}As_x)$,[6] $La(Fe_{1-x}Si_x)_{13}$ and their hydrides,[7] Ni_2MnGa (Heusler alloys),[8] $Fe_{49}Rh_{51}$,[9] and the manganites ($RE_{1-x}M_xMnO_3$ where M=Ca, Sr, and Ba).[10] Giant MCE is obtained by combining several contributions to the total entropy variation, e.g., the giant MCE of $Gd_5(Si_2Ge_2)$ results of the coupling between a first-order structural transition (lattice, ΔS_{lat}) and a second-order magnetic transition,[4] for $Fe_{49}Rh_{51}$ it is the coupling between electronic (ΔS_e) and magnetic transitions.[9] However, first-order transition and strong magnetocrystalline coupling present several disadvantages: the highly hysteretic and hard magnetic behavior reduces the efficiency of the cooling process since it gives rise to energy losses, and the structural change promotes cracks nucleation and propagation which may cause severe damages of the refrigerant material during cycling. Furthermore, the refrigeration capacity or the relative cooling power (RCP) of a solid refrigerant is also a function of the temperature range over which the transition takes place; this quantity is often taken as the full width at half maximum (FWHM) of $\Delta S_M(T)$, δT_{FWHM}.[11] First-order transitions are sharp which reduces the operating temperature range and the RCP. Another important parameter to evaluate the performance of magnetic refrigerants is the shift in temperature of the magnetic transition point ΔT_{pt} in a magnetic field.[12,13] ΔT_{pt} is usually less significant for a magnetic transition superimposed on a first-order structural transition.

Because of these, the main direction that we have chosen to investigate concerns materials with second-order magnetic transition only, and high MCE properties. Metallic glasses display a very unique combination of properties interesting for applications in magnetic refrigeration: (i) they are soft magnets with second-order magnetic transition, reduced coercivity, and high permeability, (ii) the transition temperature can be tailored by either composition tuning and annealing,[14–16] i.e., composite effect due to the formation of nanocrystallites into the amorphous matrix, and (iii) the mechanical and corrosion resistances are highly improved in the glassy state.[17]

We have produced a series of RE-based metallic glasses[18–20] and we report here the magnetic properties and magnetocaloric effect of a Gd-based glass with a nominal composition $Gd_{60}Al_{10}Mn_{30}$ containing nanocrystallites of Gd. Its MCE properties are compared with other reference materials from the literature.

The alloy composition was designed based on topologic and thermodynamic criteria described elsewhere[18] to ensure a good glass forming ability. Furthermore, no ternary compound containing more than 33.3 at. % of gadolinium is reported in the Gd–Al–Mn system. Master alloy with the nominal composition was prepared by melting high-purity elements in a levitation furnace under argon atmosphere. The

[a]Author to whom correspondence should be addressed. Electronic mail: gorsse@icmcb-bordeaux.cnrs.fr.

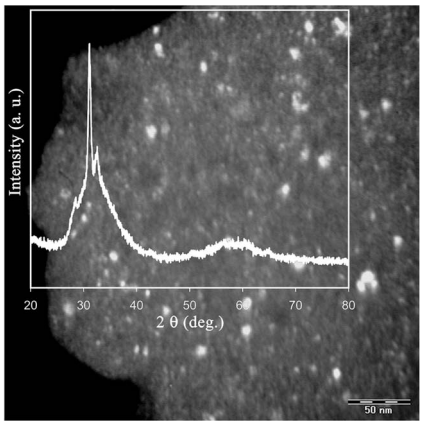

FIG. 1. TEM dark field micrograph of the melt-spun $Gd_{60}Al_{10}Mn_{30}$ ribbon showing nanocrystallites of less than 10 nm is size embedded into the amorphous matrix. X-ray diffraction pattern is also shown in the inset figure.

amorphous alloy was produced in the form of ribbons by single-roller melt-spinning technique with a circumferential speed of 30 m/s.

The structural state of the melt-spun ribbons was examined by x-ray diffraction (inset of Fig. 1). In addition to two diffuse diffraction bands, peaks from hexagonal Gd are present which indicates a mixture of amorphous and crystalline phases. This result is confirmed by transmission electron microscopy (TEM) showing nanocrystallites of 10 nm in diameter embedded into an amorphous matrix (Fig. 1).

Plot of the ratio H/M (H is the applied field and M the magnetization) as a function of the temperature at $\mu_0 H = 0.1$ T (Fig. 2), shows that the behaviour of the $Gd_{60}Al_{10}Mn_{30}$ nanocomposite can be reproduced by a Curie–Weiss law for temperature above 300 K, with a paramagnetic Curie temperature $\theta_P = 238$ K and an effective moment of $5.8\mu_B$. Given the effective moment of Gd^{3+} ions ($7.94\mu_B$), it is found an effective magnetic moment of $3.45\mu_B$ for the Mn^{2+} ions. At lower temperature (<300 K), the susceptibility starts to deviate from the Curie–Weiss temperature.

In Fig. 3, the zero-field-cooled (ZFC) and field-cooled (FC) magnetization curves $M(T)$, for an applied field $\mu_0 H = 0.1$ T, show three second-order magnetic transitions at $T = 278$, 250, and 149 K.

The thermal event at 278 K is very close to the Curie temperature of pure Gd, i.e., 293 K, and is attributed to the ferromagnetic ordering of Gd moments in the Gd nanocrystallites.

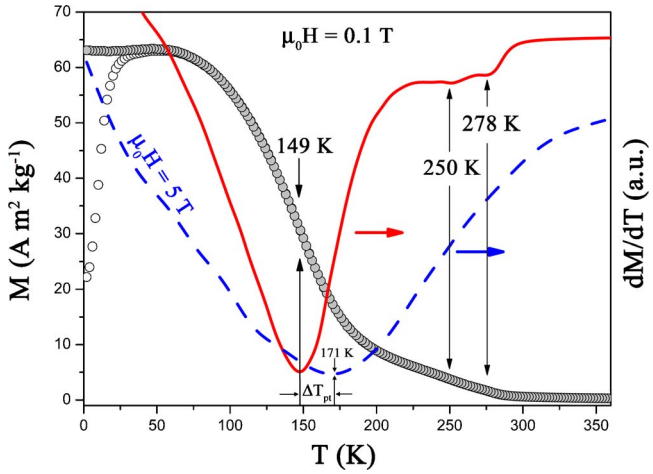

FIG. 3. (Color online) Temperature dependence of the ZFC (open symbols) and FC (full symbols) magnetization curves at $\mu_0 H = 0.1$ T for the $Gd_{60}Al_{10}Mn_{30}$ nanocomposite. The derivatives of the magnetization, dM/dT vs T, at 0.1 and 5 T are shown by the solid (red) and dashed (blue) lines, respectively.

The second event at 250 K can be attributed to the interaction between nanocrystallites of Gd, i.e., the ordering of the magnetic clusters.[21]

The magnetic transition at 149 K is broad, which is typical of structurally disordered phase in which exchange interactions fluctuate in space as a result of the variation of local environments and distances, and can be attributed to the magnetic ordering of the amorphous matrix. As shown in the inset of Fig. 2, the $Gd_{60}Al_{10}Mn_{30}$ nanocomposite behaves as a soft magnet with negligible coercivity and remanence, and a high relative permeability of 4×10^6.

ΔS_M is shown in Fig. 4 as a function of the temperature and the applied field. ΔS_M was calculated from the isothermal $M(H)$ curves (inset of Fig. 4) using the Maxwell formula,[22]

$$\Delta S_M = \int_0^H (\partial M/\partial T)_H dH. \quad (1)$$

Due to the amorphous matrix and multiple second-order magnetic transitions related to the presence of Gd nanocrystallites, the peak entropy is very broad with temperatures

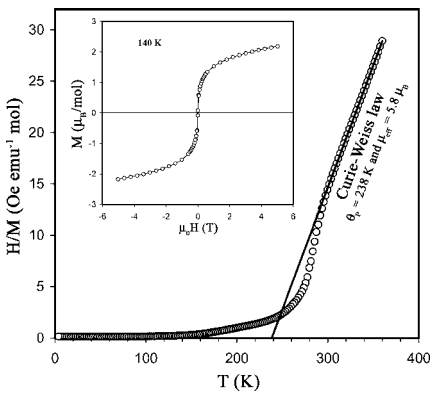

FIG. 2. H/M ratio plot of the $Gd_{60}Al_{10}Mn_{30}$ nanocomposite at $H = 1000$ Oe ($\mu_0 H = 0.1$ T). The line represents the Curie–Weiss law at high temperatures ($R^2 = 0.999$). The figure inset shows the magnetic hysteresis loop $M(H)$ at 140 K.

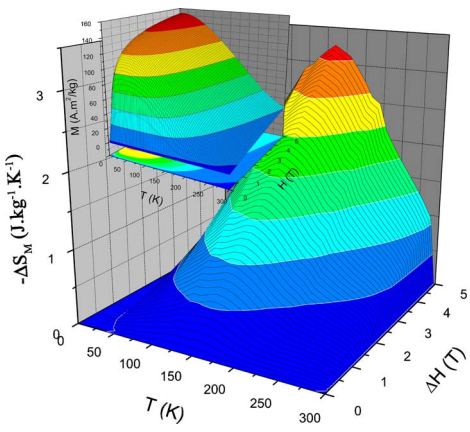

FIG. 4. (Color online) Temperature and field dependences of the magnetic entropy change and magnetization (inset figure) of the $Gd_{60}Al_{10}Mn_{30}$ nanocomposite.

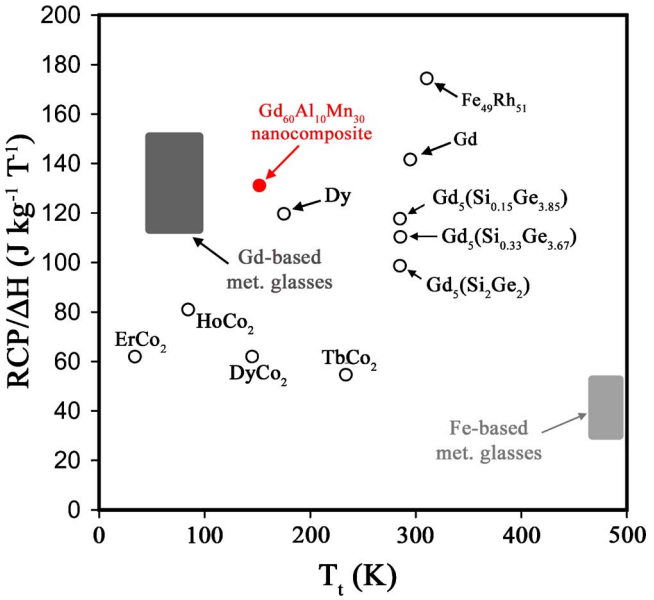

FIG. 5. (Color online) Normalized relative cooling power, RCP/ΔH, plotted against the transition temperature, T_t, for some high MCE crystallized compounds (Ref. 13), metallic glasses,[25–27] Gd,[29] Dy,[30] and the $Gd_{60}Al_{10}Mn_{30}$ nanocomposite from the present work.

ranging from 20 to 300 K. The peak entropy change ΔS_M^{peak} shift from 149 to 171 K when $\mu_0 H$ increases from 0.1 to 5 T, and is related to the magnetic transition of the amorphous phase. ΔS_M^{peak} reaches −1.4 and −3.3 J kg^{-1} K^{-1}, δT_{FWHM} is 150 and 200 K, and the resulting refrigeration capacity, RCP$=\Delta S_M^{\text{peak}}\ \delta T_{\text{FWHM}}$, is 210 and 660 J kg^{-1}, for a field change of 2 and 5 T, respectively.

Indirect determination of ΔT_{ad} can be performed from the measured magnetization and temperature dependence of the heat capacity,[23,24]

$$\Delta T_{\text{ad}}(T;0 \rightarrow H) = -\frac{T}{C_0(T)}\Delta S_M(T;0 \rightarrow H). \quad (2)$$

The temperature dependence of the heat capacity at zero field, $C_0(T)$, was measured by a relaxation method using a Quantum Design physical properties measurement system (PPMS). At the peak entropy change, $C_0(T)$ $=285$ J kg^{-1} K^{-1}, which gives $\Delta T_{\text{ad}}=0.8$ and 2 K for ΔH $=2$ and 5 T, respectively.

Despite lower peak values of ΔS_M and ΔT_{ad}, compared to giant MCE materials, the $Gd_{60}Al_{10}Mn_{30}$ exhibits higher RCP than most of the crystalline materials with first-order transition. Such high RCP results of the extension of the MCE over a large temperature range (of the order of 100 K) due to the amorphous nature of the matrix and the presence of nanocrystallites; in comparison, MCE of crystalline materials with first-order transition is concentrated over a narrow range (of the order of 10 K). In the so-called intermediate temperature range between 80 and 250 K, MCE of RM_2 Laves phases and manganites have been extensively studied. For working temperature around 180 K, the best magnetic refrigerant material is pure Dy.[12,13,28] As shown in Fig. 5, where the normalized RCP/ΔH is plotted against the transition temperature T_t for some crystallized compounds and metallic glasses, the $Gd_{60}Al_{10}Mn_{30}$ nanocomposite has a higher refrigerant capacity than pure Dy at comparable working temperature.

One can also note the high value of ΔT_{pt} (=22 K for $\Delta H=5$ T) which compares well with other giant MCE crystallized materials.[13]

In conclusion, the $Gd_{60}Al_{10}Mn_{30}$ nanocomposite, a material with second-order magnetic transitions resulting of the amorphous nature of its matrix and the presence of nanocrystallites, exhibits a refrigeration capacity comparable to the best crystallized materials with a magnetic transition superimposed on a first-order structural transition. This high refrigerant efficiency combined with a very soft magnetic behavior (very high permeability and negligible coercivity) and a wide operating temperature range make the $Gd_{60}Al_{10}Mn_{30}$ nanocomposite an attractive candidate as magnetic refrigerants around 150 K, where very few materials are currently available.

This work was supported by the CNRS through the Exploratory program RM2 PE1.8-13.

[1]E. Warburg, Ann. Phys. **13**, 141 (1881).
[2]J. Glanz, Science **279**, 2045 (1998).
[3]K. A. Gschneidner, Jr., V. K. Pechersky, and A. O. Tsokol, Rep. Prog. Phys. **68**, 1479 (2005).
[4]V. K. Pecharsky and K. A. Gschneidner, Phys. Rev. Lett. **78**, 4494 (1997).
[5]H. Wada and Y. Tanabe, Appl. Phys. Lett. **79**, 3302 (2001).
[6]O. Tegus, E. Bruck, K. H. J. Buschow, and F. R. De Boer, Nature (London) **415**, 150 (2002).
[7]A. Fujita, S. Fujieda, and K. Fukamichi, Appl. Phys. Lett. **81**, 1276 (2002).
[8]F.-X. Hu, B.-G. Shen, and J.-R. Sun, Appl. Phys. Lett. **76**, 3460 (2000).
[9]M. P. Annaorazoy and S. A. Nikitin, J. Appl. Phys. **79**, 1689 (1996).
[10]W. Chen, W. Zhong, D. L. Hou, R. W. Gao, W. C. Feng, M. G. Zhu, and Y. W. Du, J. Phys.: Condens. Matter **14**, 11889 (2002).
[11]K. A. Gscheidner, Jr., V. K. Pecharsky, A. O. Pecharsky, and C. B. Zimm, Mater. Sci. Forum **315-317**, 69 (1999).
[12]A. M. Tishin and Yu. I. Spichkin, *The Magnetocaloric Effect and Its Applications* (IOP, Bristol, 2003).
[13]A. M. Tishin, J. Magn. Magn. Mater. **316**, 351 (2007).
[14]A. Hernando, I. Navarro, and P. Gorria, Phys. Rev. B **51**, 3281 (1995).
[15]V. Franco, J. S. Blazquez, C. F. Conde, and A. Conde, Appl. Phys. Lett. **88**, 042505 (2006).
[16]V. Franco, J. S. Blazquez, M. Millan, J. M. Borrego, C. F. Conde, and A. Conde, J. Appl. Phys. **101**, 09C503 (2007).
[17]J. R. Scully, A. Gebert, and J. H. Payer, J. Mater. Res. **22**, 303 (2007).
[18]G. Orveillon, O. N. Senkov, J.-L. Soubeyroux, B. Chevalier, and S. Gorsse, Adv. Eng. Mater. **9**, 483 (2007).
[19]G. Orveillon, B. Chevalier, and S. Gorsse, J. Alloys Compd. (to be published), doi: 10.1016/j.jallcom.2007.10.078.
[20]S. Gorsse, G. Orveillon, and B. Chevalier, J. Appl. Phys. **103**, 044902 (2008).
[21]L. Wang, J. Ding, H. Z. Kong, Y. Li, and Y. P. Feng, Phys. Rev. B **64**, 214410 (2001).
[22]A. H. Morrish, *The Physical Principles of Magnetism* (Wiley, New York, 1964), Chap. 3.
[23]V. K. Pecharsky and K. A. Gschneidner, Jr., J. Magn. Magn. Mater. **200**, 44 (1999).
[24]V. K. Pecharsky, K. A. Gschneidner, Jr., A. O. Pecharsky, and A. M. Tishin, Phys. Rev. B **64**, 144406 (2001).
[25]Q. Luo, D. Q. Zhao, M. X. Pan, and W. H. Wang, Appl. Phys. Lett. **89**, 081914 (2006).
[26]V. Franco, J. M. Borrego, C. F. Conde, A. Conde, M. Stoica, and S. Roth, J. Appl. Phys. **100**, 083903 (2006).
[27]T. D. Shen, R. B. Schwarz, J. Y. Coulter, and J. D. Thompson, J. Appl. Phys. **91**, 5240 (2002).
[28]S. M. Benford, J. Appl. Phys. **50**, 1868 (1979).
[29]S. Y. Dan'Kov, A. M. Tishin, V. K. Pecharsky, and K. A. Gscheidner, Jr., Phys. Rev. B **57**, 3478 (1998).
[30]S. A. Nikitin, A. M. Tishin, S. F. Savchenkova, Yu. I. Spichkin, O. D. Chistykov, S. V. Redko, and Yu. A. Nesterov, J. Magn. Magn. Mater. **92**, 405 (1991).